Accurate Antenna Characterisation at VHF/UHF Frequencies with Plane Wave Generator Systems

V. Schirosi, F. Saccardi *AMTA Senior*, A. Giacomini *AMTA Senior*, F. Scattone, L. Scialacqua, A. Diamanti, E. Tartaglino, L.J. Foged *AMTA Fellow*
MVG Italy, Via Castelli Romani, 59, Pomezia, ITALY
lars.foged@mvg-world.com

N. Gross, S. Anwar *AMTA Member*, E. Kaverine
MVG Industries
13 Rue du Zéphyr, 91140 Villejust, FRANCE
nicolas.gross@mvg-world.com

P.O. Iversen *AMTA Fellow*, E. Szpindor *AMTA Senior*
MVG Orbit Advanced Technologies Inc.
650 Louis Drive, Suite 100, 18974 Warminster, PA, USA
peri@orbitfr.com

***Abstract* — This paper aims to compare the capabilities and advantages of Plane Wave Generators (PWG) and Compact Antenna Test Ranges (CATR) of similar physical size, operating in the VHF/UHF frequency range. The primary focus of this study is on the benefits of utilizing the PWG at such low frequencies for antenna and device characterization. We demonstrate that the PWG offers a superior approximation to the far-field (FF) plane wave condition in the quiet zone (QZ) compared to similar sized CATR systems. The better performance of the PWG at these frequencies is expected, as this is an unusual frequency range for an optical system such as CATR. Due to the efficient focusing properties of the array, the PWG exhibits significantly reduced side wall illumination and thus resulting reflections within the anechoic chamber. This translates into a substantial improvement in overall measurement uncertainty. The CATR system requires specific edge treatment, such as serrations or rolled edges, which increase the overall system's size and associated cost while reducing the effective area of the reflector. Our findings suggest that at low frequencies such as VHF/UHF, a PWG-based solution can be designed to comparable performance to the CATR system while maintaining a considerably smaller size and lower cost, making it an attractive alternative for low frequency antenna testing at in anechoic environments.**

I. INTRODUCTION

The growing interest in Over-The-Air (OTA), or End-to-End, testing of devices has driven the development of alternative indirect far-field measurement systems based on Plane Wave Generators (PWGs). A PWG, comprising an antenna array with suitable lattice and complex excitation, approximates a plane wave condition at a close distance, facilitating testing in Far Field (FF) conditions at reduced and convenient distances [1-6]. This paper explores the manifold advantages of PWGs compared to other antenna testing systems.

For example, Near Field (NF) systems measure radiated signals on a closed surface at a reduced distance, requiring a software-based NF-to-FF transformation with phase-coherent samples [7]. NF systems are more suitable for tests with a phase reference, such as passive measurements, although techniques have been developed to enable a full recovery of phase information for OTA testing purposes. Conversely, direct-FF ranges excel in such testing, requiring only amplitude data, but necessitate longer measurement distances and thus a more costly testing environments [2].

The PWG shares numerous similarities with the classic Compact Antenna Test Range (CATR) in their shared goal of approximating a plane wave condition at a near field distance within a limited test volume known as the Quiet Zone (QZ), where the Device Under Test (DUT) is positioned. However, the systems differs in their approach. The CATR is an optical system that employs one or more reflectors to collimate the spherical wave from a feed antenna, creating a cylindrical QZ volume. In contrast, the PWG relies on phased array technology, enabling it to concentrate the radiated energy within a spherical QZ volume. This distinction allows the PWG to be more compact compared to a CATR as it does not require a feed antenna and achieves the plane wave condition at a significantly shorter distance.

An important aspect to consider in antenna testing systems is the link budget, directly impacting dynamic range. Under ideal lossless conditions, a PWG can achieve superior performance to a CATR. However, in the final link budget, it is important to consider the losses introduced by the distribution network of the PWG. These losses can mitigate the previously observed advantage, necessitating careful and precise design considerations to fully exploit the capabilities of the PWG.

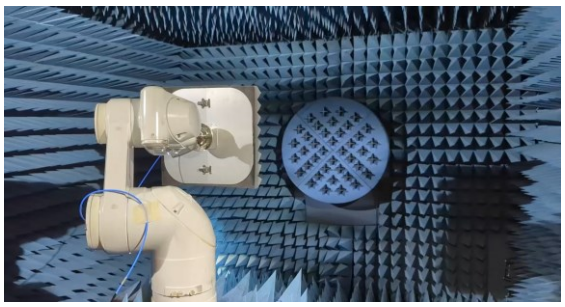

Figure 1. Example of 40 element PWG [600-6000 MHz] based on robotic positioner with QZ of 60cm [5].

II. PLANE WAVE GENERATOR SYSTEM

A Plane Wave Generator (PWG) is an advanced engineering system leveraging phased array technology. It consists of an array of radiating elements, each with optimized complex coefficients (amplitude and phase), enabling the approximation of a plane wave, thus a Far Field (FF) condition within a spherical Quiet Zone (QZ) volume situated in the Near Field (NF) region of the array. The grid arrangement of the array is generally regularly symmetric for symmetric QZ, adopting strategies such as squared, circular, hexagonal, etc as illustrated in Figure 2 [8].

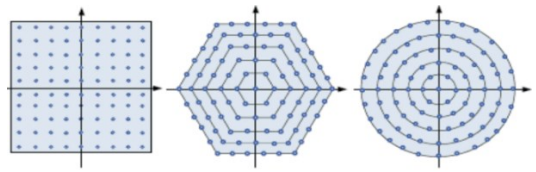

Figure 2. Examples of array grids in a PWG

At higher frequencies, the circular grid has traditionally been employed as the baseline for PWG systems. However, for lower frequencies, such as VHF/UHF band, mechanical considerations become paramount due to the substantial physical dimensions of the involved antennas. In light of this, exploring alternative grid configurations like squared or hexagonal layouts becomes pertinent. These alternative grids offer valuable opportunities to reduce mechanical complexities of the system while maintaining comparable electrical performance.

Figure 3. Plane Wave Generator systems for millimeter-wave applications in personal communication [9].

Recent millimeter-wave PWG systems exemplify circular grid symmetry [9] as shown in Figure 3. In these systems, the radiating elements and their spacing are electrically large (2λ at the lowest frequency), making circular grid symmetry advantageous for simplifying the feeding network. However, at sub-6GHz frequencies, such as systems presented in [5] features elements that are much closer together (0.3λ at the lowest frequency). In such cases, the element coupling becomes significant, leading to preference for regular grid configuration, such as square or hexagonal. The use of a regular grid ensures that the coupling has a symmetrical effect on the embedded element pattern, preventing degradation of the Quiet Zone (QZ) performance of the PWG.

The design parameters of the PWG, include the number of radiating elements, their relative spacing, dimensions, and absolute position. This is commonly referred to as element density. Other parameters such as the composition of sub-arrays and complex weights, are intricately linked to the achievable quality of the Far-Field (FF) approximation within the spherical QZ and the achievable power density. Additionally, having dual polarization capabilities is highly desirable for simultaneous measurement of two orthogonal polarizations. The PWG's cross-polar performance is dependent on the angular polarization purity of the individual elements within the QZ view angle, which is typically around 10°.

For carefully miniaturized elements, the closest spacing achievable is approximately 0.3λ/0.4λ. If wide frequency band operation is a requirement, the aperture sampling or element spacing at the highest design frequency becomes the limiting factor for PWG performance [3], [4], [10]. When the PWG-to-QZ spacing is electrically large, at least greater than the PWG diameter, the array supports wider spacing between the elements. However, for practical designs, this sets the upper to lower frequency limit at around 10:1. Notably, examples of such designs can be found in [5].

The radiating elements are excited with different complex weights according to two main excitation schemes:

- Independent excitation: a different complex weight is applied to each induvidual element of the array. This allows also for the generation of assymetric QZ coverage.
- Sub-array excitation: sub-arrays, such as full or partial rings can be considered as they often have same complex exitation due to the symmetry of the PWG.

The Beam Forming Network (BFN) plays a critical role in the system, as it is responsible for distributing the complex weights to each element. The amplitude variation of the coefficients can be achieved using low noise/power amplifiers, which increase the relative signal levels, or attenuators, where the reference ring is set to 0dB attenuation, and all others are normalized accordingly. The phase variation of the coefficients is generally realized through programmable phase shifters.

The frequency dependance of the optimum complex coefficients is not high. For this reason it is often advantageous to apply a BFN capable of wide band operation. This can be achieved by using phase macthed cables and components and wide band amplitude and phase shifters as described in [5].

A typical BFN is composed of 3 main blocks:

- A first divider stage (one or more), that allows to split the input signal in N lines (where N is the number of rings) and excite simultaneosly the elements within a sub-array.
- On each sub-array channel, a programmable amplitude and phase shifter allows to generate a complex coefficient that will be applied to all elements of the sub-array.
- Then, another division stage right after the programmable amplitude and phase shifter that splits the signal in M_n lines (where M_n is the number of elements in the sub-array *n*).

The relative excitation of sub-arrays is digitally controlled by the programmable amplitude and phase shifter and responsible for the quality of the plane wave approximation in the QZ. The amplitude and phase shifters can be fully digital as in [9] or digitally controlled analog components as in [5]. The difference is the ease of implementation and availble dynamic range of the exitation coefficients achievable by a digital solution at the expense of the bandwidth limitation by the digital convertion. The fully analog solution, can be digitally controlled and designed to cover the full frequency range supported by the analog components such as couplers, dividers, cables etc.

III. Synthesis Strategy

The process of PWG optimization involves finding the optimum weights on the array elements, subject to constraints imposed by the BFN, by minimize an objective function. The commonly adopted objective function aims to minimize the maximum deviation, both in amplitude and phase, between the synthesized field at stations defining the QZ and the desired field. The desired QZ in front of the PWG is defined by a number of discrete points known as synthesis stations.

The radiated field from each array element is determined at these stations, which can be achieved through direct measurement by a probing strategy directly in the test range, numerical modeling of the array elements, or post-processing of measured data. Examples: In [5] these field were found by measurements in a spherical NF system of the PWG and post-processing, in [9] these fields were determined by QZ probing both onsite and in a measurement system.

The optimum coefficients to achieve the best approximation to FF condition within the QZ varies with frequency as the coefficients have to compensate for the discrete sampling of the aperture by the radiating elements. The frequency dependance is not strong and a further design constraint can be applied to fix the coeffcients for sub-bandwidth or the entire band of the PWG if changing coefficients in a frequency sweep is deemed undesirable.

The PWG exitation synthesis problem for the four main optimisation parameters to achieve the desired QZ can be summarised as:

- Field uniformity on the QZ area. Amplitude and phase deviation from the approximation to plane wave condition in the QZ. For PWG, the approximation is flat over the QZ avoiding the well-know taper from optical system such as CATR [2].
- Discrete frequencies or full/sub-bandwidth optimisation of complex coefficients. In some cases, discrete optimum coefficients for each frequency is considered undesirable for the PWG operation.
- Maximize ratio of radiated power inside to outside the QZ and in particular to limit the anechoic chamber illumination. This is also equivalent to maximize the NF directivity [10], [17].
- Minimize the dynamic of the amplitude excitation coefficients that in turn maximize the NF gain[17]. If BFN is based on attenuators, this requirement is needed to minimize losses and hence increase the dynamic range.

An alternative objective function has been implemented for PWG optimization, as discussed in [5] and [11]. This approach uses un-normalized array coefficients in the optimization, with an additional constraint to optimize the total energy falling within the QZ defined by the stations. This formulation offers several advantages, as it effectively minimizes the fields outside the QZ without introducing further stations to the problem. Additionally, it transforms the optimization into a well-behaved real non-linear min-max problem, enabling classical optimization algorithms to efficiently determine the optimum array coefficients while considering the BFN constraints.

IV. Example VHF/UHF Plane Wave Generator

The system presented in this paper can be efficiently scaled to operation at frequencies within the VHF/UHF bands, covering a 10:1 frequency range. All dimensions of the array are scaled to λ_0, the wavelength at the lowest operational frequency f_0. The PWG comprises an array of around 100 dual-polarized radiating elements, strategically distributed across the radiating surface. The elements can be miniaturized to fit into the dense array arrangement. The elements can be conveniently mounted on the chamber wall or allocated on a fixed/movable support structure within the chamber. A typical system following this strategem is shown in Figure 4.

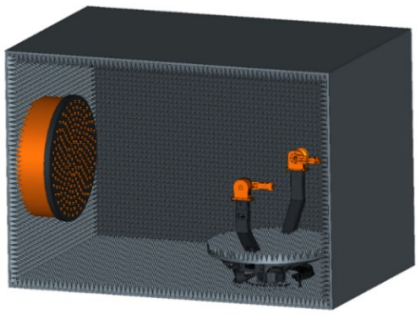

Figure 4. Example of PWG system designed for operation in VHF/UHF frequency range.

The chamber absorber lining must be sufficient to accommodate operation at the lowest design frequency. As will be illustrated later, the PWG effeciently focus the radiation into the QZ in the first 3:1 f_0 frequency range, with very little illumination of the chamber. As frequency increases beyond $3f_0$, the array will continue to ensure excellent QZ illumination, albeit with the emergence of grating lobes due to array sampling (Figure 5.). Consequently, these lobes will start illuminating the chamber's lateral surfaces, including the ceiling, floor, and walls. The chamber lateral surfaces can therefore conviently be lined with absorbers of dimensions less than λ_0. The wall behind the Antenna Under Test (AUT) will experience strong illumination, fortunately at normal incidence, which optimizes absorber performance. To minimize reflections into the QZ, it is recommended to cover this wall with an specific anechoic arrangement and larger absorber dimensions such as at least λ_0.

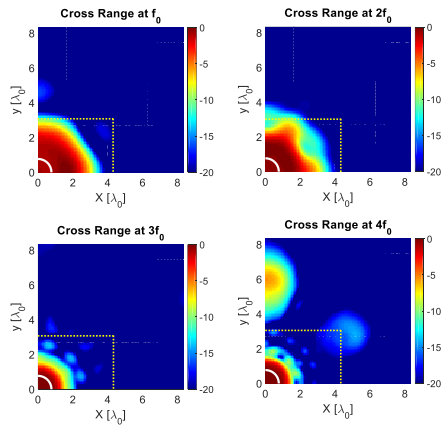

Figure 5. Example of free space cross-range PWG field distribution at f_0, $2f_0$, $3f_0$ and $4f_0$ frequencies. Chamber limits are included in yellow to appreciate illumination of lateral surface at higher frequencies.

Main components and typical dimensions of a generic VHF/UHF frequency range PWG system are the following:

- PWG with 10:1 frequency bandwidth.
- Array of ~100 miniaturazied, dual polarised radiating elements, embedded in absorbing material, with minimum 0.3-0.4 λ_0 spacing on a surface of diameter ~4-5λ_0.
- Distance PWG array to center of QZ: 5-7 λ_0.
- Variable/fixed (spherical) QZ size depending on the design criteria and frequency. At the highest frequency, $10f_0$, the QZ size is limited by the array sampling to ~1.5λ_0. It can be as hight as ~3λ_0 at the lowest frequency f_0.
- Anechoic chamber dimention: ~7λ_0x7λ_0x10λ_0 (WxHxL).
- Absorber lining: ~0.5λ_0 size absorbers on lateral surfaces such as celing, floor and walls. ~λ_0 size absorbers (at least) on the wall behind the antenna under test.

V. Comparison of a PWG to a CATR System

We compare the simulated performance of comparable sized PWG and CATR. The CATR is simplified as we consider only the contribution from the reflector suppression disturbances such as the direct radiation by the feed in the numerical simulation. In the comparison, we consider normalized frequency and dimensions with respect to the lowest frequency of the PWG, denoted f_0, and corresponding wavelength λ_0.

The PWG is a hexagonal array of approx. 4λ_0 diameter with 85 elements. The array is divided in 11 sub-arrays (or rings) and each element of every individual ring has uniform amplitude and phase. The spherical QZ is 6.4λ_0 from the aperture of the array.

The radiating elements are miniaturized elements used by MVG in their multi probe system with directivity ranging from 4dBi at f_0 to 10dBi at $5f_0$. The element coupling is accounted by full wave simulation of embedded elements [12].

The CATR in the comparison is a standard floor-fed system with dimension and edge treatment to operate from $4f_0$. This system fits the same anechoic environment as the PWG it is compared to. The focal length of the system is 6.3λ_0 and the cross-section of the rolled-edge reflector is 3.7λ_0 x 4.3λ_0. The CATR is thus slightly larger than the PWG (4λ_0) vs diagonal 5.7λ_0. The CATR QZ is situated 8.3λ_0 from the reflector, slightly further than the PWG. To operate the CATR at f_0 frequency it is feed by a quad-ridge horn with 0.7λ_0 aperture. The gain of the quad-ridge horn ranges from 4dBi to 10dBi in the considered $f_0 - 5f_0$ band. The CATR has been simulated with a MoM-based full-wave solver [12]. Only the radiation from the reflector surface currents have been considered in the analysis, neglecting the direct radiation from the feed to the QZ. The feed position of the CATR has been optimized to improve the QZ uniformity.

The S_{21} downrange vertical maps of the CATR have been computed with the SWE-based transmission formula [1] and are reported for four frequencies: f_0, $2f_0$, $3f_0$ and $5f_0$ in Figure 6. The white circle indicates the position of the QZ. Following the methodology described in [13] and [17], the coupling between the CATR (represented by its own spherical wave coefficients) and an ideal Hertzian dipole has been computed for all the reported YZ pairs of points in front of the reflector. It is highlighted that, since no normalization has been applied to the field computed by the full-wave solver, the computed coupling also accounts for the feed illumination efficiency. As can be seen the field distributions are significantly different at the reported frequencies. At $5f_0$ the constant flux of energy that one would expect from a CATR system is indeed generated. By moving to lower frequencies, the flux is significantly degraded. At f_0 and $2f_0$ for example it is evident that the reflector is electrically too small to properly transform the spherical wave front radiated by the feed to a plane wave front.

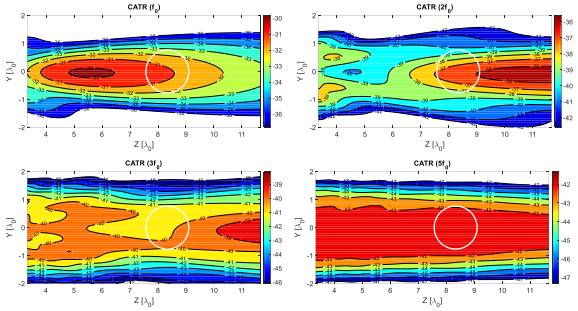

Figure 6. Downrange S_{21}-map distributions of the considered 17m-reflector CATR.

The S_{21} downrange vertical maps provided by the PWG have been computed with the same method based on the transmission formula and are reported for four frequencies: f_0, $2f_0$, $3f_0$ and $5f_0$ in Figure 7.

The white circle indicates the position the spherical QZ of diameter 1.5λ_0 at 6.4λ_0 distance in front of the PWG. The field distributions, computed at the same frequencies of the CATR, significantly differ from the latter. The near field focusing effect achieved with the synthesis process at the chosen QZ can be appreciated at each frequency. Especially at lower frequencies, the superior performance of PWG against the CATR is highlighted.

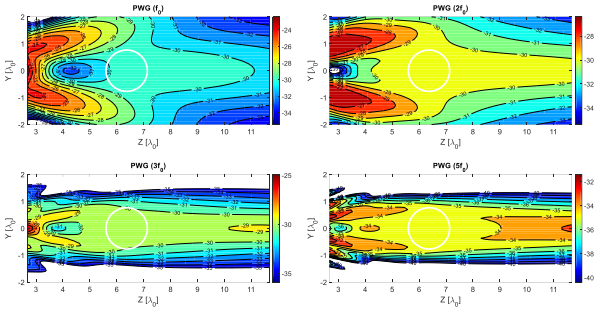

Figure 7. Downrange S_{21}-map distributions of the considered 12-meter diameter PWG.

The uniformity of the QZ for both the PWG and CATR systems, which are comparable in physical size are illustrated in Figure 8. The quantification is based on the worst-case peak-to-peak amplitude and phase variation observed on $1.5\lambda_0$ diameter spheres, centered at distances $8.3\lambda_0$ from the reflector and $6.4\lambda_0$ from the PWG. It is evident from the results that the PWG exhibits superior performance, particularly at the lowest frequencies.

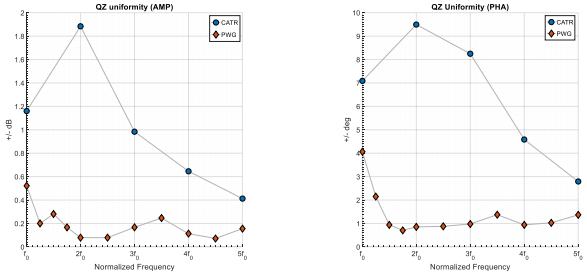

Figure 8. Comparison of amplitude (left) and phase (right) QZ uniformity in ideal conditions.

It should be noted that the QZ performance of both systems is achieved under ideal conditions. In installed systems, various factors can potentially degrade the performance of both the PWG and CATR systems. For low-frequency CATR systems, other contributing factors affecting QZ quality include feed direct radiation to the test zone and possible system misalignment. In contrast, critical aspects to be considered in a low-frequency PWG system involve the coupling between the array elements and potential errors in the distribution network. Addressing these factors diligently is crucial to achieve optimal QZ performance in both systems. One major concern, common to both systems and especially critical at low frequencies, is chamber reflections that are ignored in the above comparison.

To assess chamber performance, we conducted a comparison between the PWG, CATR, and a horn (e.g., a quad-ridge horn with a $0.7\lambda_0$ aperture, similar to the one used to feed the CATR). These evaluations took place within a lateral wall anechoic chamber configuration measuring $7\lambda_0$ by $7\lambda_0$. The analysis considered a flat absorber reflectivity of -30dB at normal incidence, while neglecting the influence of the back and front walls of the chamber. To determine the equivalent QZ reflectivity for all systems, we employed a first-order ray tracing technique [17]. This allows a comparative evaluation of each system within a given specified chamber environment. The results are shown in Figure 9. The equivalent QZ reflectivity of the system is generally better or equivalent to the absorber reflectivity due to the focusing effect of all systems [15], [16]. The equivalent QZ reflectivity by the PWG is clearly superior to the CATR and horn in particular at the lower frequencies. The reflectivity only becomes comparable around $4f_0$ where PWG grating lobes specular illuminates the chamber lateral walls.

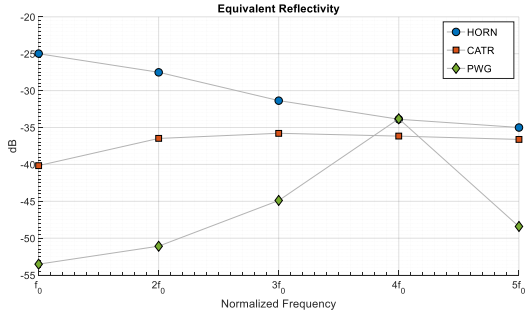

Figure 9. Comparison of equivalent anechoic chamber reflecivity using a horn, a CATR and PWG.

The coupling between the PWG and the CATR with an ideal Hertzian dipole in the center of their respective QZ is shown in Figure 10. The coupling has been evaluated using the transmission formula and the simulation of the PWG and CATR respectively [17]. The coupling computation is reported in ideal losses conditions for better comparison. It is observed that the PWG has higher coupling than the CATR.

The NF directivity of a system can be computed by evaluating the radiation pattern at a specific distance. It quantifies the amount of power radiated in a particular direction with respect to an isotropic radiator [17].

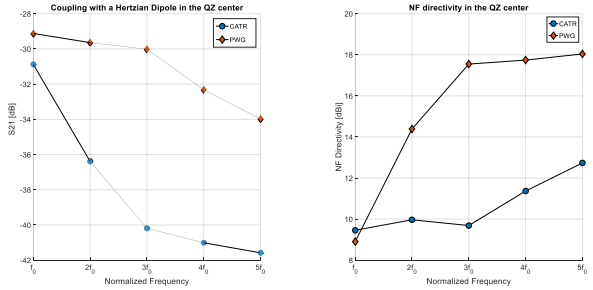

Figure 10. Comparison of (partial) link-budget: Emulated coupling with a Hertzian dipole in the QZ center (left); NF directvity in the QZ center (right).

In Figure 10. (right), we present the NF directivity of both the PWG and CATR at the distance from their respective QZ. Notably, the PWG, despite being slightly smaller than the CATR, exhibits significantly higher directivity within the QZ. This characteristic also accounts for the PWG's superior coupling factor compared to the CATR. Importantly, higher directivity implies lower illumination of the test environment, leading to attenuated stray signals entering the QZ. This feature further contributes to the overall enhanced performance of the PWG over the CATR [14][15][16].

While the PWG demonstrates a higher signal power level, it is essential to account for loss introduced by the distribution network in the final link budget. The loss have the potential to mitigate the observed advantage, emphasizing the need for meticulous and accurate design considerations to fully exploit the capabilities of the PWG. To achieve optimal performance, it becomes crucial to minimize the dynamic range of the array excitation coefficients during the synthesis process. By doing so, we can effectively manage the impact of losses and ensure efficient operation of the PWG system.

VI. Measurement Performance Estimation

Using the transmission formula technique [17] the measurement of a horn antenna (e.g., a quad-ridge horn with a $0.7\,\lambda_0$ aperture, like the CATR feed) in a reflection free environment has been determined. The results are shown in Figure 11. at f_0 (left) and $2f_0$ (right) frequencies. The equivalent noise level indicates the error introduced in the measurement from the imperfect approximation to FF condition in the QZ of the systems. Surprisingly, the superior performance of the PWG is less evident at f_0 but significantly better at all frequencies between f_0 and $4f_0$ as can be expected.

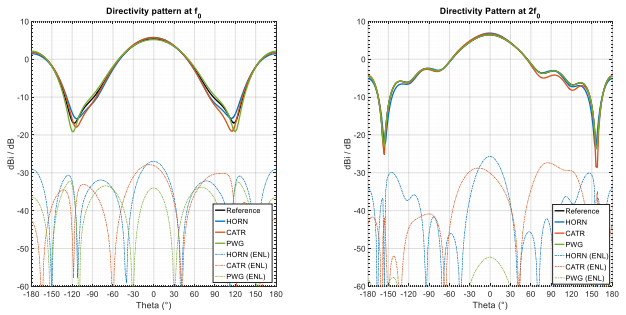

Figure 11. Measurement of horn antenna at f_0 (left) and $2f_0$ (right) frequencies by PWG, CATR and horn in reflection free enviroment (free space) Phi=0° cut.

VII. Conclusions

In this paper, we report a comprehensive comparison of the capabilities and advantages between Plane Wave Generators (PWG) and Compact Antenna Test Ranges (CATR) specifically targeting applications in the VHF/UHF frequency range. We specifically focused on setups with similar physical dimensions.

The PWG exhibits a lower frequency range approximately four times lower than that of the CATR. Moreover, its strong array-based focusing effect rendered it less sensitive to the chamber environment compared to the CATR. However, in the crossover frequency range, both the CATR and PWG demonstrated comparable performances and showed similar insensitivity to the absorber lining of the chamber. At higher frequencies, beyond 10 times the lower frequency of the PWG, the CATR's optical system properties offered superior performance. Consequently, the PWG can be considered an excellent complementary technique to the CATR, primarily due to its ability to cover the lower frequency ranges within the same chamber size.

Acknowledgement

The authors would like to acknowledge the valuable input and discussions with people and organizations outside MVG.

References

[1] J. E. Hansen (ed.), Spherical Near-Field Antenna Measurements, Peter Peregrinus Ltd., on behalf of IEE, London, United Kingdom, 1988

[2] IEEE Std 149-2021 “IEEE Recommended Practice for Antenna Measurements”

[3] A. Capozzoli, C. Curcio, G. D’Elia, A. De Simone, A. Liseno, "An optimized approach to plane wave synthesis", Proc. of the 29th Annual Antenna Measurem. Tech. Ass. Symp, 2008.

[4] A Capozzoli, C Curcio, G D'elia, A Liseno, G Ianniello, and P Vinetti, "Effective 2D generalised plane wave synthesizers: Experimental validation", Proc. of the 30th Annual Antenna Measurem. Tech. Ass. Symp, 2009.

[5] F. Scattone, D. Sekuljica, A. Giacomini, F. Saccardi, L. J. Foged A. Scannavini, N. Gross, P. O Iversen, “Plane Wave Generator for Direct Far-field Over-The-Air Testing of Devices”, AMTA 2018, 4-9 November, Williamsburg, VA, USA

[6] H. Bartko, A. Tankielun and B. Derat, "New Measurements Concept of Electrically Large Active Antenna Systems in Compact Test Chambers," 2019 8th Asia-Pacific Conference on Antennas and Propagation (APCAP), Incheon, Korea (South), 2019

[7] IEEE Std 1720-2012 “Recommended Practice for Near-Field Antenna Measurements”

[8] K. Karad, V. Hendre, “Review of Antenna Array for 5G Technology Using mmWave Massive MIMO”, Recent Trends in Electronics and Communication, vol 777. Springer.

[9] F. Scattone, D. Sekuljica, A. Giacomini, F. Saccardi, A. Scannavini, E. Kaverine, S. Anwar , N. Gross, P. O Iversen, L. J. Foged “Preliminary Assesment of Millimeter Wave Plane Wave Generator For 5G Device Testing”EuCAP 2021, 22-26 March 2021, Düsseldorf, Germany

[10] O. M. Bucci, M. D. Migliore, G. Panariello, and D. Pinchera, "Plane-Wave Generators: Design Guidelines, Achievable Performances and Effective Synthesis," *IEEE Transactions on Antennas and Propagation*, vol. 61, no. 4, pp. 2005-2018, Apr. 2013.

[11] P. E. Frandsen and S. B. Sørensen, "Formulations of the contoured beam array antenna minmax optimization problem", Proceedings of the *1994 Progress in Electromagnetics Research Symposium*, European Space Agency, Noordwijk, The Netherlands, Jul. 1994.

[12] Dassault Systems, CST Studio Suite 2023

[13] R. T. Sánchez, F. Saccardi, A. Giacomini, M. A. Saporetti, P. Moseley and L. J. Foged, "Measurement of Low Frequency Antennas in Indoor Reflective Environments with the Synthetic Probe Array Technique" EuCAP *2022*, 27 March – 1 April, Madrid, Spain

[14] F. Saccardi, R. Tena-Sanchez, E. Tartaglino, A. Giacomini, L. J. Foged, P. Moseley, L. Rolo “Measurement of VHF Satellite Antennas using the Synthetic Probe Array Technique” Internation Symposium on Measurements and Networking, Padua, Italy, 18-20 July, 2022

[15] F. Saccardi, R. Tena-Sanchez, E. Tartaglino, A. Giacomini, L. J. Foged P. Moseley, L. Rolo “Testing of a 60 MHz Cubesat in an Electrically Small Environment with the Synthetic Probe Array Technique”, AMTA 2022, October 9-14, Denver, CO, USA

[16] Per C. Hansen; F. H. Larsen “Suppression of reflections by directive probes in spherical near-field measurements” IEEE Transactions on Antennas and Propagation, VOL. AP-32, NO. 2, February 1984

[17] F. Saccardi, A. Giacomini, L. J. Foged “Accurate Evaluation of Antenna Measurement Range Performance with the SWE Transmission Formula” AMTA 2023, October 8-13, Seattle, WA, USA